DMD Fast Forward. Published on November 30, 2016 as DOI: 10.1124/dmd.116.072371
This article has not been copyedited and formatted. The final version may differ from this version.

Impact of organic cation transporters (OCT-SLC22A) on differential diagnosis of intrahepatic lesions

Authors

Michele Visentin, Belle V. van Rosmalen, Christian Hiller, Matthanja Bieze, Lia Hofstetter, Joanne Verheij, Gerd A. Kullak-Ublick, Hermann Koepsell, Saffire S.K.S. Phoa, Ikumi Tamai, Roelof J. Bennink, Thomas M. van Gulik, Bruno Stieger

Affiliations

Department of Clinical Pharmacology and Toxicology, University Hospital Zurich, University of Zurich, Switzerland (M.V., C.H., L.H., G.A. K.-U., B.S.)

Department of Surgery, Academic Medical Center, University of Amsterdam, Amsterdam, The Netherlands (B.V. v.R., M.B., T.M. v.G.)

Department of Nuclear Medicine, Academic Medical Center, University of Amsterdam, Amsterdam, The Netherlands (R.J.B.)

Department of Radiology, Academic Medical Center, University of Amsterdam, Amsterdam, The Netherlands (S.S.K.S.P.)

Department of Pathology, Academic Medical Center, University of Amsterdam, Amsterdam, The Netherlands (J.V.)

Department of Molecular Plant Physiology and Biophysics, Julius-von-Sachs-Institute, University of Würzburg, Germany (H.K.)

Faculty of Pharmaceutical Sciences, Institute of Medical, Pharmaceutical and Health Sciences, Kanazawa University, Japan (I.T.)

DMD Fast Forward. Published on November 30, 2016 as DOI: 10.1124/dmd.116.072371
This article has not been copyedited and formatted. The final version may differ from this version.

Running Title

OCTs and [^{18}F]fluoromethylcholine uptake

Corresponding authors

Bruno Stieger, Ph. D., University Hospital Zurich, Raemistrasse 100, CH-8091 Zurich. Phone: +41 446343169, Fax: +41 442554411, E-mail: bruno.stieger@uzh.ch.

Thomas M. van Gulik, M.D. Ph. D., Academic Medical Center, Department of Surgery. P.O. Box 22700, NL-1100 DD Amsterdam, Phone: +31 205665570, Fax: +31 206976621, E-mail: t.m.vangulik@amc.nl.

Text Pages: 27

Tables: 2

Figures: 8

Supplementary Files: 1

References: 49

Abstract Word Count: 250

Introduction Word Count: 443

Discussion Word Count: 809

Abbreviations: 4-(4-(dimethylamino)-styryl)-N-methylpyridinium iodide, ASP^+; choline kinase, CK; fluoromethylcholine, FCH; focal nodular hyperplasia, FNH; hepatocellular adenoma, HCA; hepatocellular carcinoma, HCC; organic cation transporter, OCT; positron emission tomography, PET; tetraethylammonium bromide, TEA.

DMD Fast Forward. Published on November 30, 2016 as DOI: 10.1124/dmd.116.072371
This article has not been copyedited and formatted. The final version may differ from this version.

Abstract

Positron emission tomography (PET) using the cationic compound [^{18}F]fluoromethylcholine (FCH) enhances the sensitivity for non-invasive classification of hepatic tumours due to peculiar patterns of accumulation. The underlying transporters are not known. We aim to identify the carriers mediating uptake of FCH in liver and to correlate their expression pattern with PET intrahepatic signal distribution to clarify the role of membrane transporters in FCH accumulation. FCH transport was characterized in cells overexpressing organic cation transporters (OCTs). OCT mRNA levels were determined in different types of hepatic lesions and correlated with FCH PET signal intensity. Additionally, OCT1 and OCT3 protein was analyzed in a subset of patients by Western blotting. HEK293 cells overexpressing OCT1, OCT2 or OCT3 showed higher intracellular levels of FCH in comparison to wild-type cells. mRNA levels of OCT1 paralleled protein levels and were significantly downregulated in hepatocellular carcinoma (HCC), hepatocellular adenoma (HCA) and, to a lesser extent, in focal nodular hyperplasia (FNH) compared to matched non-tumour tissues. In 3 patients with HCA, the FCH PET signal intensity was reduced relative to normal liver. This correlated with the simultaneous downregulation of OCT1 and OCT3 mRNA. In another patient with HCA, lesion and surrounding tissue did not show a difference in signal, coinciding with downregulation of OCT1 and upregulation of OCT3. Therefore, OCT1 is very likely a key transporter for the accumulation of FCH in the liver. The data supports the hypothesis that the varying expression levels of OCT1 and OCT3 in focal liver lesions determine FCH PET signal intensity.

Introduction

The overlapping enhancement patterns and non-typical appearance at the common radiologic modalities can complicate the noninvasive diagnosis of hypervascularized hepatic lesions, especially for the distinction between focal nodular hyperplasia (FNH), hepatocellular adenoma (HCA) and hepatocellular carcinoma (HCC) (Hamm et al., 1994; Grazioli et al., 2005). Differentiation of these entities is crucial for appropriate management (Stoot et al., 2010; Bieze et al., 2014).

Focal lesions and diffuse liver diseases display altered expression levels of the main hepatic membrane transporters resulting in peculiar disposition patterns of the gadolinium-based hepatobiliary contrast agents that improve the accuracy of magnetic resonance imaging (Grazioli et al., 2005; Nilsson et al., 2013; Nilsson et al., 2014; Pastor et al., 2014). Likewise, unique accumulation of the positron emission tomography (PET) tracer [^{18}F]fluoromethylcholine (FCH) enhances the sensitivity for the detection and differentiation of focal liver lesions (Talbot et al., 2006; Talbot et al., 2010; van den Esschert et al., 2011; Kwee et al., 2015). The molecular features of the varying FCH accumulation in hepatic lesions are unknown.

FCH is an analogue of choline, precursor of phosphatidylcholine, betaine and acetylcholine (ACh) (Pelech and Vance, 1984; Kwee et al., 2007). Carrying a positive charge FCH requires transport systems for cellular entry. Because choline kinase (CK), which phosphorylates choline to phosphocholine in the first committed step of the Kennedy pathway, is often upregulated in tumours, the enhanced accumulation of FCH is thought to be a mere consequence of an increased choline metabolism (Glunde et al., 2015). However, some studies failed to correlate the total choline levels in tumours and uptake of [^{11}C]choline measured by PET (Utriainen et al., 2003; Yamaguchi et al., 2005). One study comparing the total choline contents between HCC and matched non-cancerous liver tissues revealed that the

majority of the HCC had lower choline levels than the matched non-tumour tissues, in apparent discrepancy with the generally higher FCH accumulation by HCC at PET analysis (Talbot et al., 2006; Wang et al., 2008; Talbot et al., 2010; Kwee et al., 2015).

The varying accumulation of FCH between different types of hypervascularized liver lesions might be the result of heterogeneous expression levels of relevant membrane transporters. The uptake of choline in the liver is likely mediated by members of the organic cation transporters, notably OCT1, and the choline transporter-like proteins (CTLs) (Koepsell, 2013; Tamai, 2013; Inazu, 2014).

Here we combined a functional transport study to identify the transporters expressed in the liver mediating the uptake of FCH with a retrospective analysis of their mRNA and protein expression pattern in patients with different types of liver lesions. Subsequently, we investigated whether changes of transporter expression correlated with the intrahepatic FCH accumulation at the PET analysis.

Patients and Methods

Patients and Liver Tissues

All the procedures followed were in accordance with the ethical standards of the responsible committee on human experimentation and with the Helsinki declaration. The local medical ethic committee approved the study and written informed consent was obtained from all patients (age ≥ 18) before entering the study. Patients with suspicion of FNH or HCA larger than 2 cm with no history of malignancy or chronic liver disease and with normal serum alpha-fetoprotein were included. Patients with proven HCC or suspicion of HCC were included when surgical treatment was performed. More information about patient characteristics is listed in table 1.

DMD Fast Forward. Published on November 30, 2016 as DOI: 10.1124/dmd.116.072371
This article has not been copyedited and formatted. The final version may differ from this version.

A lesion was defined as HCA if it showed a hepatocellular proliferation with no cytonuclear atypia, absence of portal tracts, presence of solitary arteries and a well-developed reticulin framework (Bioulac-Sage et al., 2009). A lesion was defined as FNH if it showed a hepatocellular proliferation without cytonuclear atypia and within the lesion aberrant arterial vessels, fibrotic strands and ductular reaction with inflammation. Additional immunohistochemical staining for glutamine synthetase showed a peculiar pattern of expression. A lesion was defined as HCC if it showed cytonuclear atypia of the hepatocytes, broad trabecular and/or pseudoglandular growth and absence of portal tracts in the presence of solitary arteries. If needed, additional immunohistochemical stainings were performed (Di Tommaso et al., 2009; Shafizadeh and Kakar, 2011).

PET/CT procedure

The [^{18}F]FCH PET/CT was performed as previously described (van den Esschert et al., 2011). Briefly, a CT scan in the supine position was acquired from mid-thorax to mid-abdomen, encompassing the entire liver. The 12-channel helical CT scanning parameters were: 120 kVp, 50 mA/slice, rotation time 0.75 sec, slice thickness/interval 5.0 mm. No intravenous contrast was used. At 15 minutes after intravenous injection of 150 MBq of [^{18}F]FCH, emission scans were acquired from mid-thorax to the mid-abdomen, encompassing the entire liver.

Reagents

Fluoromethylcholine[1,2-^{3}H]chloride ([^{3}H]FCH, specific activity, 60 Ci/mmol) for in vitro studies was purchased from American Radiolabeled Chemicals (St. Louis, MO), choline chloride [methyl-^{14}C] ([^{14}C]choline, specific activity, 52 mCi/mmol), and [^{14}C]tetraethylammonium bromide ([^{14}C]TEA, specific activity 5 mCi/mmol) from Perkin Elmer (Boston, MA). Non-labeled FCH was provided by BioTrend (Köln, Germany), non-

DMD Fast Forward. Published on November 30, 2016 as DOI: 10.1124/dmd.116.072371
This article has not been copyedited and formatted. The final version may differ from this version.

labeled choline chloride and TEA by Sigma-Aldrich (St.Louis, MO). 4-(4-(dimethylamino)-styryl)-N-methylpyridinium iodide (ASP^+)) by Molecular Probes-Life Technologies (Carlsbad, Ca). All cell culture reagents were purchased from Gibco (Parsley, UK). [^{18}F]FCH for PET/CT scan was purchased from BV Cyclotron VU, Amsterdam, The Netherlands. Rabbit polyclonal anti-OCT1 (LS-C354446) and anti-OCT3 (LS-C352877) antibodies were purchased from LSBio (Seattle, WA). Anti-Protein disulphide isomerase (PDI) and horseradish peroxidase-conjugated secondary antibody were provided by Thermo Scientific (Waltham, MA).

Cell lines

Wild-type HEK293 cells were maintained in Dulbecco's modified Eagle's medium (DMEM) supplemented with 10% fetal bovine serum, 100 units/ml penicillin, 100 mg/ml streptomycin at 37°C in a humidified atmosphere of 5% CO_2. Stably transfected cell lines, previously characterized, were supplemented with Geneticin G-418 as selecting agent (Tamai et al., 1997; Tamai et al., 2001; Thevenod et al., 2013).

RNA extraction and real time reverse transcription RT-PCR

Total RNA from frozen tissue samples was extracted using the TRIzol Reagent (Life Technologies, Carlsbad, Ca). mRNAs were reverse transcribed to cDNA using random hexamers as primers and MultiScribe Reverse Transcriptase (Life Technologies, Carlsbad, Ca). The cDNA products were used as template for PCR amplification by Taqman® assay analysis (Applied Biosystems, Foster City, CA).

Isolation of human liver membrane fractions and immunoblot analysis

The isolation of a total liver membrane fraction was modified from a previously described method using 150 to 500 mg frozen liver specimens (Meier et al., 1983). After

DMD Fast Forward. Published on November 30, 2016 as DOI: 10.1124/dmd.116.072371
This article has not been copyedited and formatted. The final version may differ from this version.

homogenization of the liver tissues with a Polytron in 300 mM sucrose buffer supplemented with 1 mM phenylmethylsulfonate, 1 μM pepstatin 1 μg/ml antipain and leupeptin, the homogenates were centrifuged at $1300g_{av}$ in a Sorvall SS34 rotor. The supernatant was centrifuged for 1 h at $100000g_{av}$ in a Kontron Ultracentrifuge. The total liver membrane fractions were resuspended in 300 mM sucrose with a 25G needle and stored until use at – 80 °C. Protein samples (150 μg) were resolved on 8% (w/v) polyacrylamide gels and electroblotted onto polyvinylidene difluoride membranes (GE HealthCare, Piscataway, NJ). The membranes were blocked with 5% nonfat dry milk in phosphate saline buffer supplemented with 0.1% (v/v) Tween 20 (PBS-T), washed in PBS-T buffer, and incubated for 1 h at room temperature with anti-OCT1 or anti-OCT3 antibodies followed by probing with horseradish peroxidase-conjugated secondary antibody. Blots were developed with SuperSignal West Femto Maximum Sensitivity Substrate (Thermo Scientific, Waltham, MA) and Fusion FX7 (Vilber Lourmat, Eberhardzell, Germany). As loading control, the sample blots were stripped and reprobed with anti-protein disulphide isomerase (PDI) (Wlcek et al., 2014).

Transport Studies in Intact Cells

Uptake of radiolabeled or fluorescent compounds was measured using a protocol designed for uptake determination in cells (Schroeder et al., 1998). Cells were washed in transport buffer (136 mM NaCl, 5.3 mM KCl, 1.1 mM KH_2PO_4, 1.8 mM $CaCl_2$, 0.8 mM $MgSO_4$, 11 mM D-glucose and 10 mM Hepes/Tris, pH 7.4) at 37°C then incubated with the different tracer substrates. After extensive washing with ice-cold transport buffer, cells were solubilized and intracellular radioactivity was assessed. To measure intracellular ASP^+, the fluorescence was measured on the Twinkle LB970 microplate fluorometer (Berthold Technologies, Germany). For kinetic analysis the line was best-fit to the Michaelis-Menten equation ($V= V_{max}[S]/(K_m + [S])$). The inhibition constant (K_i) was determined from the formula: $K_{mapp} = K_m(1+[I]/K_i)$,

DMD Fast Forward. Published on November 30, 2016 as DOI: 10.1124/dmd.116.072371
This article has not been copyedited and formatted. The final version may differ from this version.

where K_{mapp} and K_m are the affinity constants of ASP^+ in the presence or absence of fluorocholine, respectively; [I] represents the extracellular concentration of fluorocholine.

Statistical Analysis

Statistical comparisons were performed using GraphPad Prism (version 5.0 for Windows, GraphPad Software). The variance in mRNA expression levels of each target gene was subjected to one-way analysis (ANOVA-test) and to a Bonferroni's test for head-to-head comparisons (post hoc comparisons). The mRNA expression level changes, in matched samples, were subjected to the two-tailed paired Student's t-test. Comparisons of transport measurements were analysed with the two-tailed Student's unpaired t-test.

Results

mRNA Expression of Genes potentially involved in Choline-partitioning into Hepatic Lesions

The expression of all potential FCH transporters and of CK expression were analyzed (Supplemental Table 1) by relative quantitative method of real time RT-PCR based on ΔCt method and expressed in Log10 scale. Based on a previous geNorm stability analysis within different liver diseases, ubiquitin C (*UBC*) gene was used in the current study as internal reference (Kim and Kim, 2003). Twelve HCC, 7 FNH and 6 HCA samples were compared with 24 healthy liver tissues. Twenty out of 24 healthy samples were from matched, non-lesion surrounding liver tissues from different patients. OCT2 and CHT1 are mainly expressed in the kidney and in the brain, respectively (Apparsundaram et al., 2000; Okuda et al., 2000; Koepsell, 2013). As expected the mRNA of these transporters was not detectable in both normal and tumorous hepatic tissues.

DMD Fast Forward. Published on November 30, 2016 as DOI: 10.1124/dmd.116.072371
This article has not been copyedited and formatted. The final version may differ from this version.

OCT1 was the only gene, within this analysis, that showed a significant degree of modulation among the 4 groups (P=0.0004) with a lower expression level in tumour tissues compared to normal tissues (Fig.1). A matched analysis was performed on the 20 patients of the study's cohort of whom the tumour and the surrounding non-tumorous, healthy tissues were available. Figure 2 is a colour-scaled representation that shows the pattern of changes for each target gene in each tumour sample relative to the mRNA expression level in the respective healthy tissue (ΔΔCt). OCT1 was significantly downregulated in HCC (7.85 ± 3.81 vs 21.23 ± 5.22, P=0.008) and in HCA (9.19 ± 1.97 vs 21.21 ± 3.17, P=0.007) (Fig.3A). Interestingly, in this analysis a pattern emerged also for OCTN1 (Fig. 3B) and CTL2 (Fig 3C). OCTN1 mRNA level in HCC was ~ 5 times that in the respective non-tumorous tissues (P=0.007), relatively stable in HCA and a trend of downregulation, albeit not significant, in FNH (P=0.23). CTL2 was slightly but significantly downregulated in HCC, unchanged in HCA and FNH. To understand whether the mRNA pattern correlated with the protein modulation, a subset of samples was quantified for protein level of OCT1 and OCT3 (Fig. 4). In table 2 the expression pattern of OCT1 and OCT3 proteins in the tumour tissues is expressed as relative to the protein level in the respective healthy tissue. It can be seen that, especially for OCT1, there was strong consistency between mRNA and protein levels.

Correlation of mRNA expression pattern and FCH PET values

Among the patients analysed, for 4 patients diagnosed with HCA, the PET/CT scan was available. These patients were part of the study previously published (van den Esschert et al., 2011). The standardized uptake value (SUV) were 7.34 ± 1.96 in the tumour and 11.69 ± 2.8 in the surrounding area (P=0.049). To investigate whether the FCH accumulation in these patients correlated with the gene expression changes, the ΔΔCt pattern of the different target genes was correlated to the tumour:normal ratio of the SUV values. For consistency, all data were expressed in Log10 scale. Three out of 4 HCA showed higher FCH signal intensity than

DMD Fast Forward. Published on November 30, 2016 as DOI: 10.1124/dmd.116.072371
This article has not been copyedited and formatted. The final version may differ from this version.

the respective surrounding normal tissues (Fig. 5). One HCA and the respective normal tissue displayed homogeneous intensity of FCH. When the PET data were correlated to the gene expression profile an interesting pattern emerged. When HCA had less FCH accumulation than the normal liver, OCT1 and OCT3 were downregulated. When HCA and normal tissue had similar FCH signal, OCT1 was downregulated but OCT3, together with OCTN2, CTL1, CTL2 and CKα were upregulated.

Impact of OCTs on the FCH net uptake in HEK293 cells

Figure 6 illustrates the time course of uptake of [^{3}H]FCH in HEK293 cells stably transfected with OCT1, OCT2 or OCT3 respectively. The transport of [^{3}H]FCH at the indicated extracellular concentration was significantly higher in OCT1-, OCT2- and OCT3-HEK293 compared with that in WT-HEK293 cells. Because OCT3 has been previously shown by two independent studies not to recognize choline as substrate (Kekuda et al., 1998; Grundemann et al., 1999), the properties of the [^{3}H]FCH OCT3-mediated transport were further studied, also with respect to the [^{14}C]choline transport. Figure 7A shows that the intracellular level of [^{14}C]choline in OCT3-expressing cells was similar to that in the wild-type cells. Figure 7B shows the OCT3-mediated influx of ASP^+ as a function of concentration in the presence or absence of 10 mM extracellular non-labeled FCH. The maximal transport capacity (V_{max}) remained unchanged, suggesting fully competitive inhibition of ASP^+ influx by non-labeled FCH. Thus, the relative affinity (K_i) of FCH for OCT3 could be computed to be 4.13 ± 0.53 mM.

Impact of OCTN1 and OCTN2 on the [^{3}H]FCH uptake in HEK293 cells

The uptake of 10 μM extracellular [^{3}H]FCH in HEK293 cells stably transfected with OCTN1 or OCTN2 was measured as the function of time. Figure 8 illustrates that the increase in intracellular [^{3}H]FCH with time was comparable in the transfected cells and in the wild-

DMD Fast Forward. Published on November 30, 2016 as DOI: 10.1124/dmd.116.072371
This article has not been copyedited and formatted. The final version may differ from this version.

type HEK293 cells suggesting no transport of [^{3}H]FCH by OCTN1 (Fig. 8A) and OCTN2 (Fig. 8B). The functionality of the transfection was assessed by measuring the uptake of the OCTN1, N2 substrate [^{14}C]TEA in transfected, and wild-type HEK293 cells (Fig. 8C).

Discussion

The present work suggests that membrane transporters and their expression levels are molecular determinants of the net uptake of FCH in liver tissue and, consequently, in the differential diagnosis of focal lesions.

FCH is rapidly cleared from the blood and retained in tumours within minutes with little redistribution suggesting that enhanced blood flow is likely to play a major role in FCH accumulation in tumours (DeGrado et al., 2001; Kwee et al., 2007; Haroon et al., 2015). However, despite the fact that hypervasculatization is a common feature of focal liver lesions, the FCH PET scan pattern varies among lesions, indicating that the hemodynamic properties of the tumour alone cannot explain such heterogeneity in FCH accumulation (Ueda et al., 1998; Trillaud et al., 2009). OCT1 is highly expressed at the basolateral membrane of hepatocytes and plays an important role in the hepatic uptake of choline (Koepsell, 2013). As previously reported, OCT1 expression level was decreased in HCC compared with normal tissues (Schaeffeler et al., 2011; Heise et al., 2012; Namisaki et al., 2014). The present work shows that such downregulation occurs also in HCA, whereas most of FNH (4/5) did not show any change. In line with this finding, FNH was reported to accumulate more FCH than the normal liver, whereas HCA was previously reported to take up less FCH than the surrounding normal tissue (Talbot et al., 2010; van den Esschert et al., 2011).

PET-imaging showed in three out of four HCA a reduced intensity and one showed a similar PET signal as the respective surrounding normal tissue. All the HCA samples were characterized by a downregulation of OCT1 suggesting a gatekeeper role in FCH accumulation in liver and providing the possible molecular explanation of the reduced

DMD Fast Forward. Published on November 30, 2016 as DOI: 10.1124/dmd.116.072371
This article has not been copyedited and formatted. The final version may differ from this version.

accumulation of FCH in HCA compared with the healthy tissue. Interestingly in the HCA sample in which FCH accumulation was comparable to that of the surrounding tissue, the OCT1 downregulation was accompanied by an upregulation of OCT3, CTL1, CTL2 and CKα (Fig. 4). The single contribution of these genes in counter-balancing the effect of the OCT1 downregulation is difficult to establish but is likely to depend on the absolute level of expression and/or their relative functional contributions.

We and others could not demonstrate OCT3-mediated transport of choline (Kekuda et al., 1998; Grundemann et al., 1999). However, FCH was here identified as an OCT3 substrate. While choline and fluorocholine are chemically similar, they appeared to be recognized differently by OCTs. This is consistent with the clinical observation that [^{11}C]choline and [^{18}F]fluorocholine accumulated differently in the different tissues, particularly liver and kidney, the main sites of expression of OCTs (Witney et al., 2012; Haroon et al., 2015).

Scarce information is available on the expression and localization of CTL1 and CTL2 in human tissues (Nair et al., 2004). In the current study the mRNA of CTL1 and CTL2 were found to be expressed in human liver, unlike in rodents in which both transporters were not detected (Traiffort et al., 2005). Whether these transporters can transport FCH should be explored.

CK catalyzes the first phosphorylation reaction in the Kennedy pathway (Pelech and Vance, 1984). This enzyme exists in mammalian cells as at least three isoforms encoded by two separate genes termed *CK-α* and *CK-β*. The active enzyme consists of either their homo- or hetero-dimeric (or oligomeric) forms (Aoyama et al., 2004). Enhanced CKα, but not CKβ, level was reported in many cancers and might be important in oncogenesis, tumour progression and metastasis (Glunde et al., 2011; Glunde et al., 2015). To our knowledge, no study has been performed on HCC yet. Here CKα mRNA expression level in tumour tissues

did not change compared with the non-tumour tissues, suggesting that CKα is likely not to play a role in the FCH signal intensity and in hepatocarcinogenesis.

Accumulation of [^{18}F]fluorodeoxyglucose (FDG) in tumours correlates with higher glucose metabolism and cell proliferation (Minn et al., 1988; Bos et al., 2002). The substantial difference in the timeframe of image acquisition between FDG (60-90 minutes) and FCH (10-15 minutes) PET scan suggests that, besides blood flow, membrane uptake rather than metabolism can determine FCH accumulation (Talbot et al., 2010; van den Esschert et al., 2011; Kwee et al., 2015). In fact, a number of studies failed to correlate intracellular accumulation of choline or FCH with choline metabolism (Utriainen et al., 2003; Yamaguchi et al., 2005; Rommel et al., 2010).

In conclusion, while, as part of a retrospective study, the number of patients studied is limited, the data give a proof of concept that OCT1 is a credible biological variable in the accumulation of FCH in intrahepatic lesions. Additionally, the study provides evidence that FCH has unique transport properties that only partially overlap with those of normal choline. A clear picture of the carriers involved in FCH uptake could help to stratify rationally the clinical situations that can profit from fluorocholine PET scan.

Acknowledgments

The authors would like to thank Stephanie Häusler for the technical assistance.

Authorship contributions

Participated in research design: Bruno Stieger, Thomas M. van Gulik and Michele Visentin.

Conducted diagnostic, surgical and experimental procedures: Michele Visentin, Belle V. van Rosmalen, Christian Hiller, Matthanja Bieze, Lia Hofstetter, Joanne Verheij, Saffire S.K.S. Phoa, Roelof J. Bennink and Thomas M. van Gulik.

Performed data analysis: Michele Visentin, Joanne Verheij, Saffire S.K.S., Phoa, Roelof J. Bennink and Bruno Stieger.

Wrote the manuscript: Michele Visentin, Belle V. van Rosmalen, Matthanja Bieze, Joanne Verheij, Gerd A. Kullak-Ublick, Hermann Koepsell, Saffire S.K.S. Phoa, Ikumi Tamai, Roelof J. Bennink, Thomas M. van Gulik and Bruno Stieger.

Reference List

Aoyama C, Liao H, and Ishidate K (2004) Structure and function of choline kinase isoforms in mammalian cells. *Prog Lipid Res* **43:**266-281.

Apparsundaram S, Ferguson SM, George AL, Jr., and Blakely RD (2000) Molecular cloning of a human, hemicholinium-3-sensitive choline transporter. *Biochem Biophys Res Commun* **276:**862-867.

Bieze M, Phoa SS, Verheij J, van Lienden KP, and van Gulik TM (2014) Risk factors for bleeding in hepatocellular adenoma. *Br J Surg* **101:**847-855.

Bioulac-Sage P, Laumonier H, Couchy G, Le Bail B, Sa Cunha A, Rullier A, Laurent C, Blanc JF, Cubel G, Trillaud H, Zucman-Rossi J, Balabaud C, and Saric J (2009) Hepatocellular adenoma management and phenotypic classification: the Bordeaux experience. *Hepatology* **50:**481-489.

Bos R, van Der Hoeven JJ, van Der Wall E, van Der Groep P, van Diest PJ, Comans EF, Joshi U, Semenza GL, Hoekstra OS, Lammertsma AA, and Molthoff CF (2002) Biologic correlates of (18)fluorodeoxyglucose uptake in human breast cancer measured by positron emission tomography. *J Clin Oncol* **20:**379-387.

DeGrado TR, Baldwin SW, Wang S, Orr MD, Liao RP, Friedman HS, Reiman R, Price DT, and Coleman RE (2001) Synthesis and evaluation of (18)F-labeled choline analogs as oncologic PET tracers. *J Nucl Med* **42:**1805-1814.

Di Tommaso L, Destro A, Seok JY, Balladore E, Terracciano L, Sangiovanni A, Iavarone M, Colombo M, Jang JJ, Yu E, Jin SY, Morenghi E, Park YN, and Roncalli M (2009) The application of markers (HSP70 GPC3 and GS) in liver biopsies is useful for detection of hepatocellular carcinoma. *J Hepatol* **50:**746-754.

Glunde K, Bhujwalla ZM, and Ronen SM (2011) Choline metabolism in malignant transformation. *Nat Rev Cancer* **11:**835-848.

Glunde K, Penet MF, Jiang L, Jacobs MA, and Bhujwalla ZM (2015) Choline metabolism-based molecular diagnosis of cancer: an update. *Expert Rev Mol Diagn* **15:**735-747.

Grazioli L, Morana G, Kirchin MA, and Schneider G (2005) Accurate differentiation of focal nodular hyperplasia from hepatic adenoma at gadobenate dimeglumine-enhanced MR imaging: prospective study. *Radiology* **236:**166-177.

Grundemann D, Liebich G, Kiefer N, Koster S, and Schomig E (1999) Selective substrates for non-neuronal monoamine transporters. *Mol Pharmacol* **56:**1-10.

Hamm B, Thoeni RF, Gould RG, Bernardino ME, Luning M, Saini S, Mahfouz AE, Taupitz M, and Wolf KJ (1994) Focal liver lesions: characterization with nonenhanced and dynamic contrast material-enhanced MR imaging. *Radiology* **190:**417-423.

Haroon A, Zanoni L, Celli M, Zakavi R, Beheshti M, Langsteger W, Fanti S, Emberton M, and Bomanji J (2015) Multicenter study evaluating extraprostatic uptake of 11C-choline, 18F-methylcholine, and 18F-ethylcholine in male patients: physiological distribution, statistical differences, imaging pearls, and normal variants. *Nucl Med Commun* **36:**1065-1075.

Heise M, Lautem A, Knapstein J, Schattenberg JM, Hoppe-Lotichius M, Foltys D, Weiler N, Zimmermann A, Schad A, Grundemann D, Otto G, Galle PR, Schuchmann M, and Zimmermann T (2012) Downregulation of organic cation transporters OCT1 (SLC22A1) and OCT3 (SLC22A3) in human hepatocellular carcinoma and their prognostic significance. *BMC Cancer* **12:**109.

Inazu M (2014) Choline transporter-like proteins CTLs/SLC44 family as a novel molecular target for cancer therapy. *Biopharm Drug Dispos* **35:**431-449.

Kekuda R, Prasad PD, Wu X, Wang H, Fei YJ, Leibach FH, and Ganapathy V (1998) Cloning and functional characterization of a potential-sensitive, polyspecific organic cation transporter (OCT3) most abundantly expressed in placenta. *J Biol Chem* **273:**15971-15979.

Kim S and Kim T (2003) Selection of optimal internal controls for gene expression profiling of liver disease. *Biotechniques* **35:**456-458, 460.

Koepsell H (2013) The SLC22 family with transporters of organic cations, anions and zwitterions. *Mol Aspects Med* **34:**413-435.

Kwee SA, DeGrado TR, Talbot JN, Gutman F, and Coel MN (2007) Cancer imaging with fluorine-18-labeled choline derivatives. *Semin Nucl Med* **37:**420-428.

Kwee SA, Wong LL, Hernandez BY, Chan OT, Sato MM, and Tsai N (2015) Chronic Liver Disease and the Detection of Hepatocellular Carcinoma by [F]fluorocholine PET/CT. *Diagnostics (Basel)* **5:**189-199.

Meier PJ, Mueller HK, Dick B, and Meyer UA (1983) Hepatic monooxygenase activities in subjects with a genetic defect in drug oxidation. *Gastroenterology* **85:**682-692.

Minn H, Joensuu H, Ahonen A, and Klemi P (1988) Fluorodeoxyglucose imaging: a method to assess the proliferative activity of human cancer in vivo. Comparison with DNA flow cytometry in head and neck tumors. *Cancer* **61:**1776-1781.

Nair TS, Kozma KE, Hoefling NL, Kommareddi PK, Ueda Y, Gong TW, Lomax MI, Lansford CD, Telian SA, Satar B, Arts HA, El-Kashlan HK, Berryhill WE, Raphael Y, and Carey TE (2004) Identification and characterization of choline transporter-like protein 2, an inner ear glycoprotein of 68 and 72 kDa that is the target of antibody-induced hearing loss. *J Neurosci* **24:**1772-1779.

Namisaki T, Schaeffeler E, Fukui H, Yoshiji H, Nakajima Y, Fritz P, Schwab M, and Nies AT (2014) Differential expression of drug uptake and efflux transporters in Japanese patients with hepatocellular carcinoma. *Drug Metab Dispos* **42:**2033-2040.

Nilsson H, Blomqvist L, Douglas L, Nordell A, Jacobsson H, Hagen K, Bergquist A, and Jonas E (2014) Dynamic gadoxetate-enhanced MRI for the assessment of total and segmental liver function and volume in primary sclerosing cholangitis. *J Magn Reson Imaging* **39:**879-886.

Nilsson H, Blomqvist L, Douglas L, Nordell A, Janczewska I, Naslund E, and Jonas E (2013) Gd-EOB-DTPA-enhanced MRI for the assessment of liver function and volume in liver cirrhosis. *Br J Radiol* **86:**20120653.

Okuda T, Haga T, Kanai Y, Endou H, Ishihara T, and Katsura I (2000) Identification and characterization of the high-affinity choline transporter. *Nat Neurosci* **3:**120-125.

Pastor CM, Mullhaupt B, and Stieger B (2014) The role of organic anion transporters in diagnosing liver diseases by magnetic resonance imaging. *Drug Metab Dispos* **42:**675-684.

Pelech SL and Vance DE (1984) Regulation of phosphatidylcholine biosynthesis. *Biochim Biophys Acta* **779:**217-251.

Rommel D, Bol A, Abarca-Quinones J, Peeters F, Robert A, Labar D, Galant C, Gregoire V, and Duprez T (2010) Rodent rhabdomyosarcoma: comparison between total choline concentration at H-MRS and [18F]-fluoromethylcholine uptake at PET using accurate methods for collecting data. *Mol Imaging Biol* **12:**415-423.

Schaeffeler E, Hellerbrand C, Nies AT, Winter S, Kruck S, Hofmann U, van der Kuip H, Zanger UM, Koepsell H, and Schwab M (2011) DNA methylation is associated with downregulation of the organic cation transporter OCT1 (SLC22A1) in human hepatocellular carcinoma. *Genome Med* **3:**82.

Schroeder A, Eckhardt U, Stieger B, Tynes R, Schteingart CD, Hofmann AF, Meier PJ, and Hagenbuch B (1998) Substrate specificity of the rat liver Na(+)-bile salt cotransporter in Xenopus laevis oocytes and in CHO cells. *Am J Physiol* **274:**G370-375.

Shafizadeh N and Kakar S (2011) Diagnosis of well-differentiated hepatocellular lesions: role of immunohistochemistry and other ancillary techniques. *Adv Anat Pathol* **18:**438-445.

Stoot JH, Coelen RJ, De Jong MC, and Dejong CH (2010) Malignant transformation of hepatocellular adenomas into hepatocellular carcinomas: a systematic review including more than 1600 adenoma cases. *HPB (Oxford)* **12:**509-522.

Talbot JN, Fartoux L, Balogova S, Nataf V, Kerrou K, Gutman F, Huchet V, Ancel D, Grange JD, and Rosmorduc O (2010) Detection of hepatocellular carcinoma with PET/CT: a prospective comparison of 18F-fluorocholine and 18F-FDG in patients with cirrhosis or chronic liver disease. *J Nucl Med* **51:**1699-1706.

Talbot JN, Gutman F, Fartoux L, Grange JD, Ganne N, Kerrou K, Grahek D, Montravers F, Poupon R, and Rosmorduc O (2006) PET/CT in patients with hepatocellular carcinoma using [(18)F]fluorocholine: preliminary comparison with [(18)F]FDG PET/CT. *Eur J Nucl Med Mol Imaging* **33:**1285-1289.

Tamai I (2013) Pharmacological and pathophysiological roles of carnitine/organic cation transporters (OCTNs: SLC22A4, SLC22A5 and Slc22a21). *Biopharm Drug Dispos* **34:**29-44.

Tamai I, China K, Sai Y, Kobayashi D, Nezu J, Kawahara E, and Tsuji A (2001) Na(+)-coupled transport of L-carnitine via high-affinity carnitine transporter OCTN2 and its subcellular localization in kidney. *Biochim Biophys Acta* **1512:**273-284.

Tamai I, Yabuuchi H, Nezu J, Sai Y, Oku A, Shimane M, and Tsuji A (1997) Cloning and characterization of a novel human pH-dependent organic cation transporter, OCTN1. *FEBS Lett* **419:**107-111.

Thevenod F, Ciarimboli G, Leistner M, Wolff NA, Lee WK, Schatz I, Keller T, Al-Monajjed R, Gorboulev V, and Koepsell H (2013) Substrate- and cell contact-dependent inhibitor affinity of human organic cation transporter 2: studies with two classical organic cation substrates and the novel substrate cd2+. *Mol Pharm* **10:**3045-3056.

Traiffort E, Ruat M, O'Regan S, and Meunier FM (2005) Molecular characterization of the family of choline transporter-like proteins and their splice variants. *J Neurochem* **92:**1116-1125.

Trillaud H, Bruel JM, Valette PJ, Vilgrain V, Schmutz G, Oyen R, Jakubowski W, Danes J, Valek V, and Greis C (2009) Characterization of focal liver lesions with SonoVue-enhanced sonography: international multicenter-study in comparison to CT and MRI. *World J Gastroenterol* **15:**3748-3756.

Ueda K, Matsui O, Kawamori Y, Kadoya M, Yoshikawa J, Gabata T, Nonomura A, and Takashima T (1998) Differentiation of hypervascular hepatic pseudolesions from hepatocellular carcinoma: value of single-level dynamic CT during hepatic arteriography. *J Comput Assist Tomogr* **22:**703-708.

Utriainen M, Komu M, Vuorinen V, Lehikoinen P, Sonninen P, Kurki T, Utriainen T, Roivainen A, Kalimo H, and Minn H (2003) Evaluation of brain tumor metabolism with [11C]choline PET and 1H-MRS. *J Neurooncol* **62:**329-338.

van den Esschert JW, Bieze M, Beuers UH, van Gulik TM, and Bennink RJ (2011) Differentiation of hepatocellular adenoma and focal nodular hyperplasia using 18F-fluorocholine PET/CT. *Eur J Nucl Med Mol Imaging* **38:**436-440.

Wang Y, Wang T, Shi X, Wan D, Zhang P, He X, Gao P, Yang S, Gu J, and Xu G (2008) Analysis of acetylcholine, choline and butyrobetaine in human liver tissues by hydrophilic interaction liquid chromatography-tandem mass spectrometry. *J Pharm Biomed Anal* **47:**870-875.

Witney TH, Alam IS, Turton DR, Smith G, Carroll L, Brickute D, Twyman FJ, Nguyen QD, Tomasi G, Awais RO, and Aboagye EO (2012) Evaluation of deuterated 18F- and 11C-labeled choline analogs for cancer detection by positron emission tomography. *Clin Cancer Res* **18:**1063-1072.

Wlcek K, Hofstetter L, and Stieger B (2014) Transport of estradiol-17beta-glucuronide, estrone-3-sulfate and taurocholate across the endoplasmic reticulum membrane: evidence for different transport systems. *Biochem Pharmacol* **88:**106-118.

Yamaguchi T, Lee J, Uemura H, Sasaki T, Takahashi N, Oka T, Shizukuishi K, Endou H, Kubota Y, and Inoue T (2005) Prostate cancer: a comparative study of 11C-choline PET and MR imaging combined with proton MR spectroscopy. *Eur J Nucl Med Mol Imaging* **32:**742-748.

Footnotes

Conflict of Interest: The authors have no conflict of interest to declare.

Financial Support: This work was supported by the Hartmann Müller foundation, Zurich, Switzerland [grant # 1705] and by the Swiss National Science foundation [grant # 310030_144195] to Bruno Stieger.

DMD Fast Forward. Published on November 30, 2016 as DOI: 10.1124/dmd.116.072371
This article has not been copyedited and formatted. The final version may differ from this version.

Figure Legend

Fig. 1 Relative Expression of choline pathway-related genes in normal liver tissue, FNH, HCA and HCC. mRNA values of the genes were normalized by the expression of the housekeeping gene *UBC* and expressed in Log10 scale and reported as scatter plot analysis with mean ± S.D. (** $P<0.01$).

Fig. 2 Colour-scaled representation of mRNA profiling of target genes in tumour samples relative to the respective non-tumour samples. The relative expression values of each target gene was measured in the tumour and in the matched healthy tissue, normalized by the expression of the housekeeping *UBC* gene and then expressed as tumour:normal ratio ($\Delta\Delta$CT). Data are reported in logarithmic scale. Blue and red colours indicate downregulation and upregulation, respectively.

Fig. 3 Pattern of OCT1, OCTN1 and CTL2 mRNA modulation in HCC, HCA and FNH in tumour samples relative to the respective non-tumour tissues. Matched plot of the mRNA level expressed as ΔCT in tumour and surrounding non-tumour samples. Data are expressed in Log10 scale.

Fig. 4 Representative immunoblot of OCT1 and OCT3 in paired tumour and normal liver tissues. Total membrane fractions (150 μg) from 8 tumour samples and the respective surrounding normal tissues were processed as described in Materials and Methods and probed with anti-OCT1 or anti-OCT3, stripped and re-probed with anti-PDI.

Fig. 5 Correlation of mRNA level changes with the FCH PET/CT scan values. Top Panel: CT and PET/CT anteroposterior axis images from 4 patients with HCA 15 min after

DMD Fast Forward. Published on November 30, 2016 as DOI: 10.1124/dmd.116.072371
This article has not been copyedited and formatted. The final version may differ from this version.

i.v. injection of 150 MBq [^{18}F]FCH. **Bottom Panel:** The relative expression data from each target gene is expressed as tumour:normal ratio (ΔΔCT). The PET ratio represents the tumour:normal SUV values. Data are reported in Log10 scale. Blue and red colours indicate downregulation and upregulation, respectively.

Fig. 6 Impact of OCT expression on the transport of [^{3}H]FCH in HEK293 cells. Time course of [^{3}H]FCH at the indicated extracellular concentrations in OCT1- (A), OCT2- (B) and OCT3-HEK293 cells. Results are the mean ± S.D. from three independent experiments.

Fig. 7 Substrate-specificity of OCT3-mediated transport. Panel A: Intracellular [^{3}H]FCH or [^{14}C]choline in WT- and OCT3-HEK293 cells was measured after 10 min incubation at 1μM extracellular concentration. **Panel B:** Kinetic analysis of the inhibition of ASP^{+} influx by non-labeled FCH. Initial uptake of ASP^{+} was assessed over 2 min in OCT3-HEK293 cells. Data were corrected for uptake in WT-HEK293 cells. ASP^{+} influx kinetics in the presence or absence of 10 mM non-labeled FCH was assessed. Results are the mean ± S.D. from three independent experiments.

Fig. 8 OCTN1- and OCTN2-mediated transport. Panel A and B: Uptake of [^{3}H]FCH at the extracellular concentration of 10 μM as a function of the time in OCTN1-HEK293 (A) and OCTN2-HEK293 cells (B). **Panel C:** Intracellular [^{14}CH]TEA in WT-, OCTN1-, OCTN2-HEK293 cells after 10 min incubation at the extracellular concentration of 10 μM. Data are the mean ± S.D. from three independent experiments.

DMD Fast Forward. Published on November 30, 2016 as DOI: 10.1124/dmd.116.072371
This article has not been copyedited and formatted. The final version may differ from this version.

Table 1. Patients and tumour characteristics.

Parameters	Category	N (%)
Age at diagnosis	< 60	15 (60)
	> 60	10 (40)
Gender	M	11 (44)
	F	14 (56)
Histopathological diagnosis	FNH	7
	HCA	6
	HCC	12
HCC Tumour Stage	pT1	3 (25)
	pT2	5 (42)
	pT3	3 (25)
	pT4	
	not available	1 (8)
HCC Etiology	HBV	2 (16)
	Alcohol	5 (42)
	Unknown	5 (42)
Tumour size (cm)	< 10	14 (56)
	> 10	11 (44)
PET	FNH	0
	HCA	4
	HCC	0

Focal Nodular Hyperplasia, FNH; Hepatitis B Virus, HBV; Hepatocellular Adenoma, HCA; Hepatocellular Carcinoma, HCC; Positron Emission Tomography, PET; Primary Tumor Stage, pT

DMD Fast Forward. Published on November 30, 2016 as DOI: 10.1124/dmd.116.072371
This article has not been copyedited and formatted. The final version may differ from this version.

Table 2. Relative changes of mRNA and protein in tumor to normal tissue expression of OCT1 and OCT3.

	OCT1		OCT3	
	mRNA	**protein**	**mRNA**	**protein**
HCA	-0.32	-0.29	-0.04	0.03
HCA	-0.30	-0.29	-0.24	-0.22
HCC	0.37	0.07	0.63	1.44
HCA	-1.07	-0.61	-0.35	-0.19
HCC	-0.20	-0.23	-0.05	-0.13
HCC	-2.49	-0.95	-0.83	0.28
HCA	-0.22	-0.94	0.75	-0.35
FNH	-0.25	-0.10	-0.34	-0.06

The relative expression values of OCT1 and OCT3 was measured in the tumour and in the matched healthy tissue. Protein disulphide isomerase (PDI) was used as loading control. Data are expressed as tumour:normal ratio and reported in logarithmic scale.

Figure 1

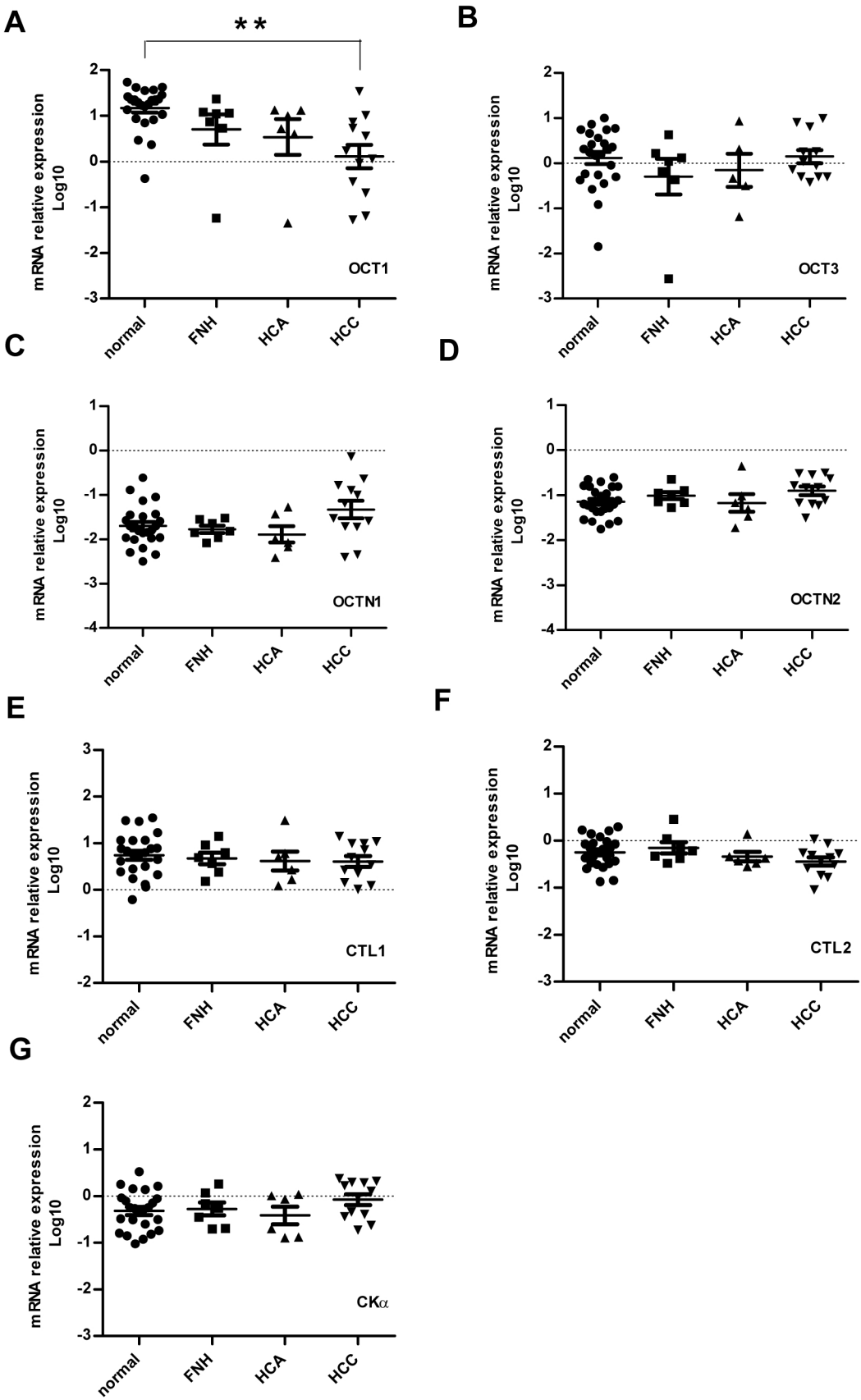
A
**
mRNA relative expression Log10
OCT1
normal
FNH
HCA
HCC
B
OCT3
C
OCTN1
D
OCTN2
E
CTL1
F
CTL2
G
CKα

Figure 2

	OCT1	OCT3	OCTN1	OCTN2	MDR1	CTL1	CTL2	CHKα	Log10
HCC	-0.95	0.47	0.43	0.29	0.03	-0.02	-0.47	0.34	5.00
HCC	-0.20	-0.05	-0.01	0.34	0.56	0.26	-0.20	0.07	4.00
HCC	-2.49	-0.83	-0.06	-0.51	-0.60	-0.71	-0.71	-0.29	3.50
HCC	-0.07	-0.05	0.21	0.31	0.44	-0.41	0.02	-0.35	3.00
HCC	-0.82	0.58	0.75	0.28	-0.41	0.24	-0.13	0.24	2.50
HCC	0.37	0.63	0.94	0.68	0.64	0.10	-0.09	0.40	2.00
HCC	-1.06	-0.49	0.91	0.44	-0.09	-0.52	0.05	0.78	1.50
HCC	-2.05	0.84	0.41	-0.02	0.39	0.23	-0.18	-0.48	1.00
HCC	-1.29	0.07	1.72	0.45	0.02	-0.05	-0.17	0.40	0.50
HCC	0.02	-0.19	0.13	0.19	-0.57	-0.22	-0.34	-0.12	0.25
HCC	-1.07	-0.47	0.44	-0.38	-0.18	-0.18	-0.23	-0.39	0.00
HCA	-0.46	-0.35	-0.36	0.11	-0.19	-0.04	0.17	0.14	-0.25
HCA	-0.32	-0.04	-0.12	0.27	0.13	-0.15	-0.12	-0.03	-0.5
HCA	-0.30	-0.24	0.17	-0.10	0.04	-0.02	-0.04	0.09	-1
HCA	-0.65	-0.74	0.21	-0.36	-0.14	-0.16	0.09	-0.08	-1.5
HCA	-0.22	0.75	0.06	0.84	0.61	0.65	0.63	0.52	-2
FNH	-0.06	0.22	-0.15	0.27	0.28	0.06	0.11	0.31	-2.5
FNH	-0.25	-0.34	-0.59	-0.44	-0.35	-0.67	-0.19	0.12	-3
FNH	-0.19	-0.73	-0.94	-0.17	-0.46	-0.58	-0.62	-0.11	-3.5
FNH	-2.79	-3.57	-0.40	0.00	-1.25	0.09	0.37	-0.45	-4
FNH	-0.89	0.68	0.45	0.38	0.75	0.75	0.26	0.51	-5

Figure 3

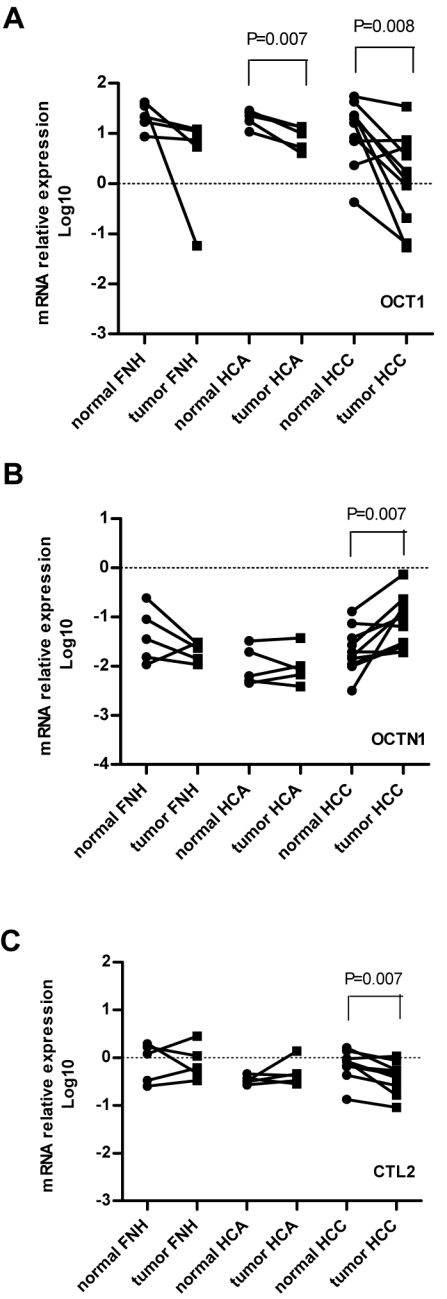
A
P=0.007
P=0.008
mRNA relative expression
Log10
OCT1
normal FNH
tumor FNH
normal HCA
tumor HCA
normal HCC
tumor HCC
B
P=0.007
mRNA relative expression
Log10
OCTN1
C
P=0.007
mRNA relative expression
Log10
CTL2

Figure 4

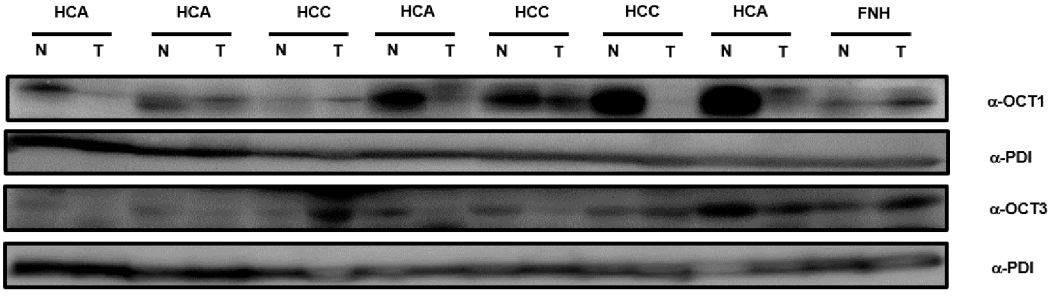
HCA
HCA
HCC
HCA
HCC
HCC
HCA
FNH
N T N T N T N T N T N T N T N T
α-OCT1
α-PDI
α-OCT3
α-PDI

Figure 5

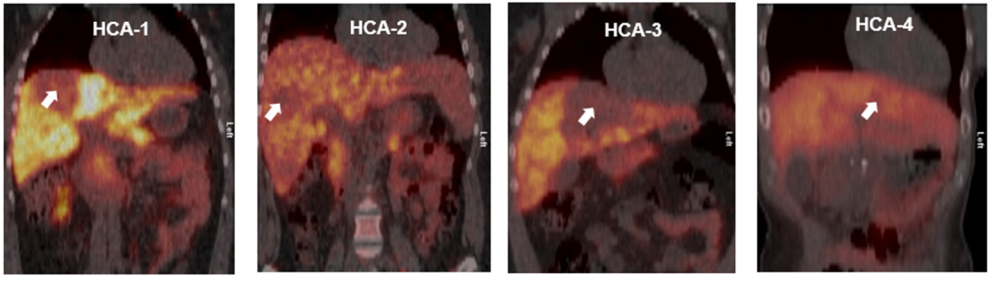

	OCT1	OCT3	OCTN1	OCTN2	CTL1	CTL2	CKα	PET
HCA-1	-0.32	-0.04	-0.12	0.27	-0.15	-0.12	-0.03	-0.25
HCA-2	-0.30	-0.24	0.17	-0.10	-0.02	-0.04	0.09	-0.23
HCA-3	-0.65	-0.74	0.21	-0.36	-0.16	0.09	-0.08	-0.38
HCA-4	-0.22	0.75	0.06	0.84	0.65	0.63	0.52	0.01

Figure 6

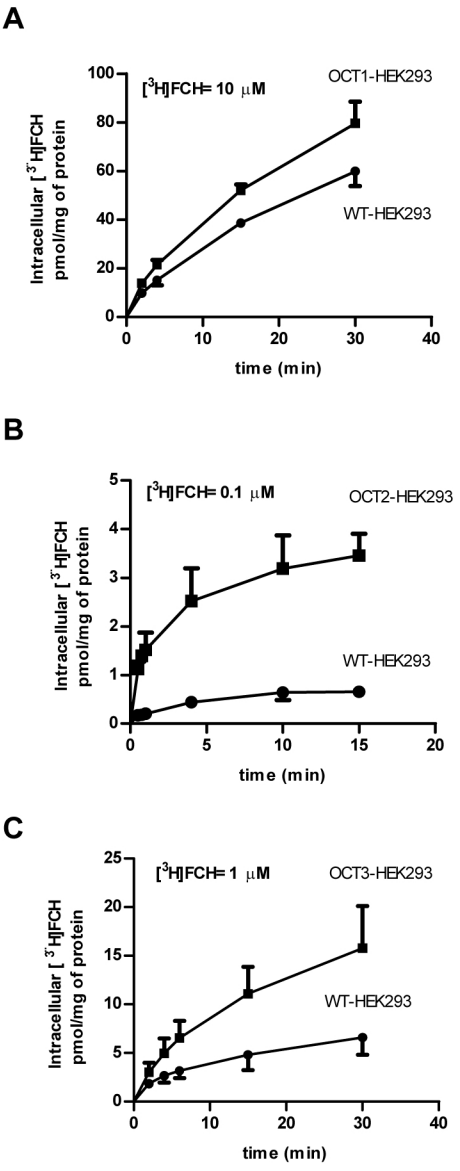
A
[3H]FCH= 10 μM
OCT1-HEK293
WT-HEK293
Intracellular [3H]FCH pmol/mg of protein
time (min)
B
[3H]FCH= 0.1 μM
OCT2-HEK293
WT-HEK293
Intracellular [3H]FCH pmol/mg of protein
time (min)
C
[3H]FCH= 1 μM
OCT3-HEK293
WT-HEK293
Intracellular [3H]FCH pmol/mg of protein
time (min)

Figure 7

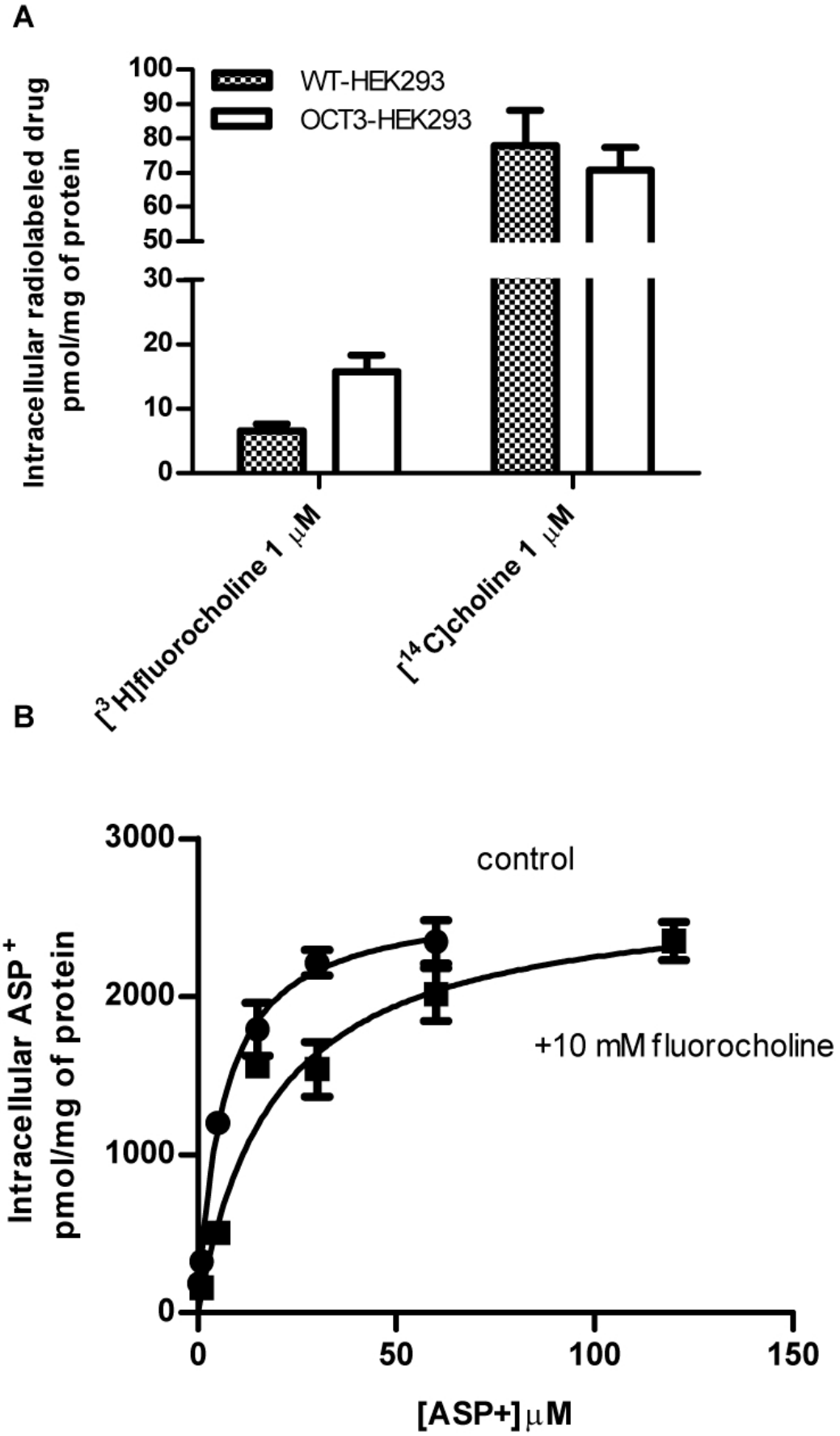
A
Intracellular radiolabeled drug
pmol/mg of protein
100
90
80
70
60
50
30
20
10
0
WT-HEK293
OCT3-HEK293
[3H]fluorocholine 1 μM
[14C]choline 1 μM
B
Intracellular ASP+
pmol/mg of protein
3000
2000
1000
0
control
+10 mM fluorocholine
0
50
100
150
[ASP+] μM

Figure 8

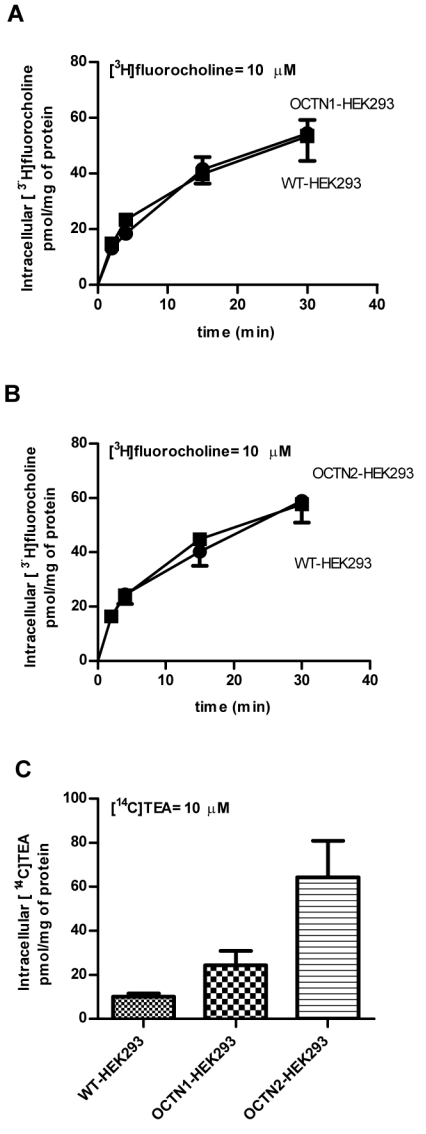
A
[3H]fluorocholine= 10 μM
OCTN1-HEK293
WT-HEK293
Intracellular [3H]fluorocholine pmol/mg of protein
time (min)
B
[3H]fluorocholine= 10 μM
OCTN2-HEK293
WT-HEK293
Intracellular [3H]fluorocholine pmol/mg of protein
time (min)
C
[14C]TEA= 10 μM
Intracellular [14C]TEA pmol/mg of protein
WT-HEK293
OCTN1-HEK293
OCTN2-HEK293